$$h \simeq \frac{K}{D}(0.56)(N_{pr} \cdot N_{gr})^{1/4}, \quad (1)$$

where K is the thermal conductivity of the water, D is the diameter of the sphere, N_{pr} is the Prandtl number and N_{gr} is the Grasshoff number. From tabulations [3] of the properties of water the quantity $N_{pr} \cdot N_{gr}$ is approximately:

$$(2) \quad N_{pr} \cdot N_{gr} \simeq 2 \times 10^4 D^3 \Delta T \, \text{cm}^{-3\,\circ}\text{C}^{-1}$$

where ΔT is the temperature difference between the ice surface and the mean temperature of the water. With $D = 2.5$ cm, $\Delta T = 45^\circ$ C, $K_{H20} = 1.5 \times 10^{-3}$ cal cm$^{-1\,\circ}$ C^{-1} sec^{-1} [4], the heat transfer coefficient becomes,

$$h \simeq 1.98 \times 10^{-2} \text{ cal cm}^{-2\,\circ}\text{ C}^{-1}\text{ sec}^{-1}. \quad (3)$$

As shown by Crandall and Ging [5] the maximum value of tensile thermal stress (σ_m) is a spherical body heated in a convection heat-transfer environment can be expressed as:

$$\sigma_m \simeq [\alpha E \Delta T/(1-\mu)]\,[2\beta/5(\beta+2)], \quad (4)$$

where ΔT is the initial temperature difference between the ice and the water, α is the coefficient of thermal expansion, E is Young's modulus, μ is Poisson's ratio and β is the Biot number defined by $\beta = Rh/K$ where R is the sphere radius, h is the heat-transfer coefficient and K is the thermal conductivity of the ice. Substitution of the following literature data for ice, $\alpha \simeq 1.13 \times 10^{-4\,\circ}$ C^{-1} [4], $E \simeq 10^{10}$ Nm^{-2}, $\mu = 0.33$ and $K \simeq 5.4 \times 10^{-3}$ cal cm$^{-1\,\circ}$ C^{-1} sec^{-1} [6], with the above value of h (Equation 3) yields:

$$\sigma_m \simeq 1.82 \times 10^7 \text{ Nm}^{-2}. \quad (5)$$

This value can be compared with a reported [6] value of the tensile strength, σ_f, of ice with $\sigma_f \simeq 1.5 \times 10^6$ Nm^{-2}, which clearly indicates that for thermal conditions and dimensions chosen for the present calculation, the thermal fracture of ice is unavoidable. A reduction in size of the ice to a diameter of approximately 0.1 cm reduces the stress to a value comparable to the fracture stress. By raising the initial temperature of the ice to its melting point, thermal fracture on heating can also be avoided, regardless of the nature of magnitude of the heat transfer involved.

Acknowledgement

The present study was conducted as part of a larger research programme on the thermomechanical and thermal properties of structural brittle materials supported by the Office of Naval Research.

References

1. W. D. KINGERY, *J. Amer. Ceram. Soc.* 38 (1955) 3.
2. J. SCHENK and F. A. M. SCHENKELS, *Appl. Sci. Res.* 19 (1968) 465.
3. R. HOSMER NORRIS, "Heat Transfer and Fluid Flow Data Book" (General Electric, Heat Transfer Division, June 1976).
4. CHARLES D. HODGMAN, Handbook of Chemistry and Physics", 36th Edn. (Chemical Rubber Publishing Co., Cleveland, 1954).
5. W. B. CRANDALL and J. GING, *J. Amer. Ceram. Soc.* 38 (1955) 44.
6. E. R. POUNDER, "The Physics of Ice" (Pergamon Press, Oxford, New York, 1965).

Received 8 August
and accepted 23 November 1978

D. P. H. HASSELMAN
Y. TREE
Department of Materials Engineering,
Virginia Polytechnic Institute and State University,
Blacksburg, Virginia 24061, USA

The angles of intersection of coarse shear bands in polystyrene

Shear bands are distinct microstructures developed during deformation of amorphous polymers such as polystyrene. They are localized regions of plastic flow and sources of shear fracture. Two different kinds of shear bands have been observed on polished surfaces after compressive deformation of atactic polystyrene [1, 2]. One appears as dark straight lines in the optical microscope and is called coarse shear bands. The other appears as diffuse zones not resolvable in the optical microscope but is revealed in the electron microscope to be thin short segments. They are called fine shear bands. While the fine bands seem to intersect at right angles, the coarse bands do not. This communication reports a set of more careful and

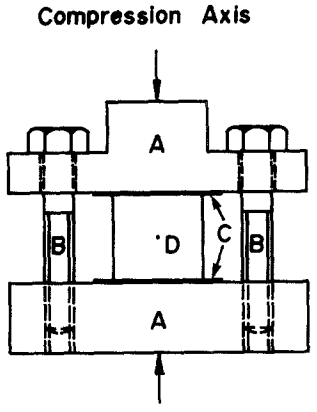

Figure 1 Steel sample holder. A, steel block; B, steel bolt; C, teflon tape; D, sample.

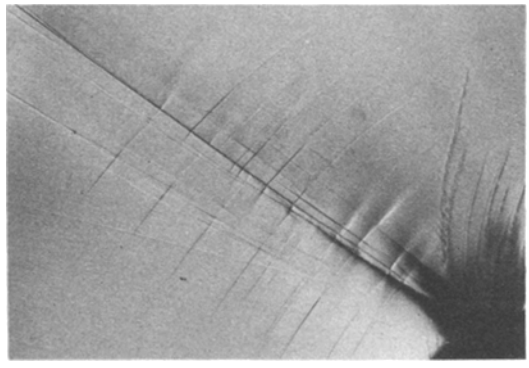

Figure 2 Coarse slip band intersection developed from the centre hole.

extensive measurements of the angles of intersection of coarse bands.

Sheets of atactic polystyrene 0.25 in. thick were obtained from Westlake Company. It was the same material as used previously [1]. As before, blocks of ~ 16 x 11 cm^2 cut from the sheets were annealed in air for about 20 h at 115° C on a glass plate coated with teflon spray. This was an attempt to remove internal stresses and moisture. The blocks were then cooled to room temperature over a period of about 7 h. Square samples of three different sizes, 0.63 x 0.63, 2 x 2, and 4 x 4 cm^2 were then cut from the blocks. A hole of 1.1 mm diameter was drilled at the centre of each sample through the thickness. The samples were then mechanically polished to 0.05 μm alumina finish. After polishing, the sample surfaces were coated with a thin layer of silver, ~ 130 Å thick, by vacuum evaporation to enhance their reflectivity.

Each sample was placed in a steel holder as shown in Fig. 1 which was then compressed in an Instron. The strain-rates used were 0.005 sec^{-1} for the 2 x 2 and 4 x 4 cm^2 sizes and 0.006 sec^{-1} for the 0.63 x 0.63 cm^2 sizes. Teflon tapes were placed between the polymer and the steel blocks in the sample holder as shown to reduce friction. As soon as the band packets were developed, the machine was stopped and the two bolts in the sample holder were tightened immediately until a sudden change in load was indicated in the Instron upon further tightening. The sample holder with the sample in it was then removed from the Instron for optical observation. The sample dimension as well as the surface morphology were preserved by the sample holder.

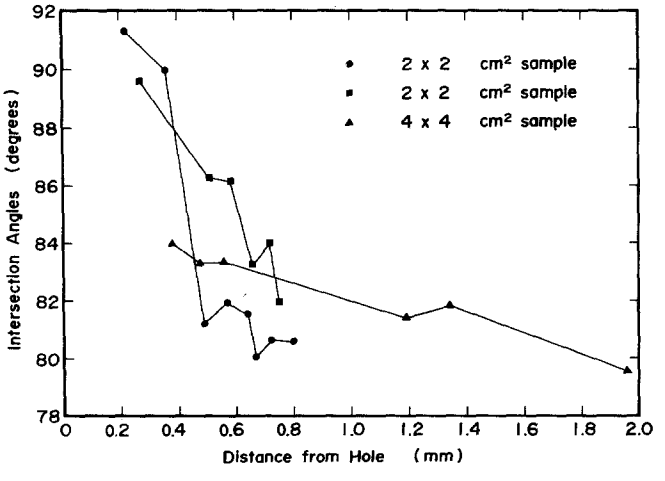

Figure 3 Variation of intersection angles with respect to distance from the hole.

The compressed sample was examined by an Olympus microscope with Nomarski contrast. The angles of intersection were measured directly by using a Unitron 10X Protractor Eyepiece, model EPTV, with vernier reading to 5 minutes of arc. Some examples of the intersections are shown in Fig. 2. Since the four slip-band packets were all originated from the centre hole, early intersections near the hole may change their angles upon further deformation. As a result, the angles near the hole are larger than those further away from the hole. This effect is shown in Fig. 3 for three samples. To avoid this complication, all angles were measured at the four outermost intersections located at the end of the four packets.

Over one hundred angles were measured for each of the three different sizes. The average values are $79.4 \pm 1.6°$, $80.1 \pm 1.5°$, and $80.3 \pm 1.5°$ for 0.63×0.63, 2×2, and $4 \times 4\ cm^2$ samples, respectively. These values can be compared with $79 \pm 1°$ reported previously [2]. The distributions are shown in Fig. 4.

These results support our contention of a normal stress effect on shear yielding of polymers [2]. The morphology of the intersections will be reported later.

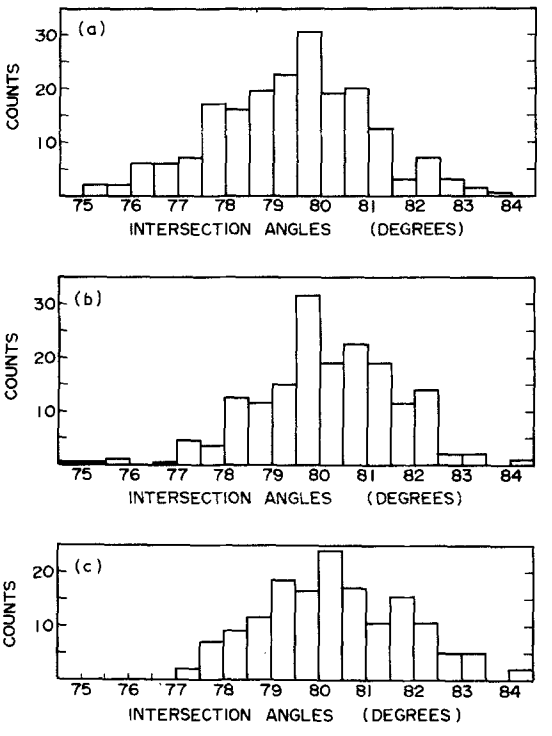

Figure 4 Distribution of intersection angles for (a) $0.63 \times 0.63\ cm^2$, (b) $2 \times 2\ cm^2$, and (c) $4 \times 4\ cm^2$ samples.

Received 21 August
and accepted 2 October 1979

BENJAMIN TAI-AN CHANG
J. C. M. LI
Materials Science Program,
Department of Mechanical and Aerospace Sciences,
University of Rochester,
Rochester, New York,
USA

Acknowledgement

This work was supported by the US Army Research Office, Research Triangle Park, North Carolina, through contract DAAG 29-76-G-0314.

References

1. J. B. C. WU and J. C. M. LI, *J. Mater. Sci.* **11** (1976) 434.
2. J. C. M. LI and J. B. C. WU, *ibid.* **11** (1976) 445.

The influence of barium and titanium dopants on the ionic conductivity and phase composition of sodium-beta-alumina

Sodium-beta-alumina is of considerable interest because its high sodium-ion conductivity makes it potentially useful in a variety of electrochemical devices, including the sodium–sulphur cell [1–3]. The crystal structure of beta-alumina consists of close-packed layers of oxygen ions with aluminium ions in the interstices in spinel-like blocks bonded together by oxygen bridges and mobile sodium ions. There are two principal forms of beta-alumina; β (hexagonal, $P6_3/mmc$) and β'' (rhombohedral, $R\bar{3}m$), which differ in the stacking sequence of the spinel blocks and the site occupancy of sodium in the conduction plane [4, 5]. The beta-alumina structure is able to accommodate a wide range of metal ions either in the conduction plane (e.g. K^+, Ag^+, Tl^+, Cu^{2+}) or in the spinel blocks (e.g. Fe^{3+}, Ga^{3+}, Co^{2+}, Mg^{2+}) [6–8]. Addition of doping ions influences the